DTI
Drug Target Insights 2025; 19: 59-70
ISSN 1177-3928 | DOI: 10.33393/dti.2025.3562
ORIGINAL RESEARCH ARTICLE

The Bushenhuoxue formula improves prothrombotic state in recurrent spontaneous abortion: network pharmacology and experimental validation

Xuan Yang[1], Shulan Su[2], Lijing Liu[3], Pan Liu[4], Maoqing Lu[5], Yinuo Wei[5], Yaqiong Gao[1]

[1]Department of Gynecology, Shanghai University of Traditional Chinese Medicine affiliated Shuguang Hospital Anhui Hospital, Anhui, Hefei - China
[2]Jiangsu Provincial Key Laboratory of Prescription High Technology Research, Nanjing University of Traditional Chinese Medicine, National and Local Joint Engineering Research Center for the Industrialization of Traditional Chinese Medicine Resources and Innovative Prescriptions, Jiangsu Province Traditional Chinese Medicine Resource Industrialization Process Collaborative Innovation Center, Nanjing, Jiangsu - China
[3]Department of Gynecology, Wuxi Traditional Chinese Medicine Hospital, Wuxi, Jiangsu - China
[4]Department of Emergency Medicine, Shanghai University of Traditional Chinese Medicine affiliated Shuguang Hospital Anhui Hospital, Anhui, Hefei - China
[5]Clinical Medicine of Traditional Chinese and Western Medicine, Anhui University of Traditional Chinese Medicine, College of Integrated Traditional Chinese and Western Medicine, Anhui, Hefei - China

ABSTRACT

Introduction: Bushenhuoxue formula is a traditional Chinese medicine formula with relatively safe clinical effects, but its mechanism in recurrent spontaneous abortion (RSA) is still unclear. Our present study used Network pharmacology an experimental validation to discuss how Bushenhuoxue formula improves prethrombotic state in RSA.
Materials and methods: The active ingredients of Bushenhuoxue formula (Drug) were acquired from our previous study. The putative targets of ZYP relevant to AS were obtained from TCMSP, Swiss Target Prediction, STITCH, DisGeNET, and Gene Cards databases. Protein-protein interactions (PPI) network, Gene Ontology (GO), and Kyoto Encyclopedia of Genes and Genomes (KEGG) analysis were conducted using the Cytoscape software. Furthermore, *in vivo* experiments were carried out for target validation in BALB/c mice, collecting placental tissue from different groups, the cell apoptosis by TUNEL assay; the pathology by HE staining; relative mRNA expression by qRT-PCR assay; relative protein expression by IHC and WB assay.
Results: Animal experiments, compared with the NC group, the AT-III, PROG, HCG, APC and t-PA concentrations were significantly depressed (P<0.05, respectively), Apoptosis cell numbers were significantly up-regulated with PI3K/AKT/HIF-1α VEGF significantly depressing (P<0.001, respectively). With Bushenhuoxue formula supplement, AT-III, PROG, HCG, APC and t-PA concentrations were significantly improved in RSA model mice; and improved pathological changes and apoptosis cell number in placenta tissues (P<0.05, respectively). However, with LY294002 supplement, the drug treatment effects were disappeared.
Conclusion: Bushenhuoxue formula improves prethrombotic state in RSA *via* stimulating PI3K/AKT/HIF-1α/VEGF pathway *in vivo.*

Keywords: Bushenhuoxue Formula, RAS, PI3K, AKT, Network Pharmacology

Introduction

Recurrent spontaneous abortion (RSA) refers to the occurrence of two or more consecutive natural miscarriages before the 20th week of pregnancy in women of reproductive age with no changes in sexual partners (1). Despite extensive research, our knowledge of the etiology of RSA remains limited, involving factors such as immune factors, endocrine factors, genetic disorders, congenital uterine developmental abnormalities, infections and coagulation function anomalies, with immune irregularities emerging as a prominent contributor (2). The disruption of the immune equilibrium due to abnormal inflammatory responses at the maternal-fetal interface is significant in fetal loss. Notably, macrophages, the principal immunoactive cells in the uterine milieu, play a crucial role in regulating the uterine immune microenvironment and mediating inflammatory responses (3). Macrophages can polarize into M1 and M2 phenotypes based on microenvironmental cues, and skewed polarization at any stage may lead to spontaneous abortion (4,5).

In recent years, the rising incidence of RSA has markedly impacted the well-being of women of reproductive age. The specific pathogenesis of RSA is not yet clear. Positive

Received: April 16, 2025
Accepted: July 14, 2025
Published online: August 19, 2025

This article includes supplementary material.

Corresponding author:
Shulan Su
email: sushulan1975@126.com

antiphospholipid antibodies are currently known immune factors related to RSA, which can affect the body's coagulation state, thrombosis, cause fetal hypoxia and death, leading to RSA (6). The treatment of Western medicine for antiphospholipid antibody positive RSA mainly focuses on anti-thrombosis, immunosuppression, and other aspects. In clinical practice, drugs such as aspirin and progesterone are often used for treatment, but their effectiveness in treating antiphospholipid antibody positive RSA is limited, and there are still problems such as low success rates of delivery (7). At present, there is no clear evidence to indicate which treatment plan is optimal for the treatment of anti-phospholipid antibody positive RSA. It is urgent to explore an efficient treatment plan for anti-phospholipid antibody positive RSA.

A previous study indicated that Bushenhuoxue formula, might enhance the condition of miscarriage-prone mice by regulating uterine and placental vasculature (8). Furthermore, the Bushenhuoxue formula has demonstrated potential in improving RSA to some extent (9). Nevertheless, the impact and underlying mechanisms of the Bushenhuoxue formula on the prothrombotic state of RSA require further elucidation. To address this gap in knowledge, the present study used network pharmacology theory and molecular docking technology to uncover the effective chemical constituents of the Bushenhuoxue formula and clarify its mechanisms involved in improving RSA. Additionally, the present study established a positive anticardiolipin antibody (ACA) mouse model of RSA, delving into the therapeutic effects and associated mechanisms of the Bushenhuoxue formula on the prothrombotic state in ACA-positive RSA mice.

Materials and methods

Network pharmacology approach

Overlapping targets between the Bushenhuoxue formula and RSA. The eight constituents of the Bushenhuoxue formula were input into the TCM Systems Pharmacology Database and Analysis Platform (TCMSP, Online). The set criteria were as follows: Oral bioavailability (OB), ≥30%; drug-likeness (DL), ≥0.18 and defaults for others to retrieve information for each constituent. Canonical SMILES data from the PubChem database (Online) were used to predict corresponding targets of every constituent in the SwissTargetPrediction database (Online) with parameters 'Homo sapiens' and probability, ≥0 to filter duplicate targets. The GeneCards database (Online) with a relevance score, ≥5 was used to identify disease-associated targets using the keyword 'RSA'. The intersection of Bushenhuoxue formula constituent targets and RSA-related targets were identified to obtain potential targets of the Bushenhuoxue formula for RSA treatment.

Construction of the 'constituent-disease target' network. The chemical constituents of the Bushenhuoxue formula and the shared targets obtained in the previous step were imported into Cytoscape (version 3.9.0) (Online). The 'constituent-disease target' network was then established. The CytoNCA tool within the Cytoscape software was used to compute degree, betweenness centrality and closeness centrality for every constituent. Chemical constituents with strong interactions with disease-related targets were identified based on centrality measurements.

Construction of the protein-protein interaction (PPI) network. The previously obtained intersected targets were input into the STRING database (Online). The settings 'multiple proteins', species 'Homo sapiens' were configured. The relevant data were then extracted and imported into Cytoscape. The CytoNCA tool was used to calculate degree, betweenness centrality and closeness centrality for every target and identify significant targets within the PPI network.

Gene ontology (GO) enrichment analysis and Kyoto Encyclopedia of Genes and Genomes (KEGG) pathway analysis of shared targets. GO and KEGG enrichment analyses were conducted using the database for annotation, visualization and integrated discovery (DAVID; Online). The GO enrichment analysis encompassed three categories: i) Biological processes (BPs); ii) molecular functions (MFs); and iii) cellular components (CCs). The results of the analyses were visualized using a bioinformatics platform (Online).

Laboratory animals. 36 BALB/c pregnant mice aged 8 weeks, with an average weight of 25±2 g, were obtained from the Animal Core Facility of Nanjing Medical University with a male-to-female ratio of 2:1.

Bushenhuoxue formula and reagents. Bushenhuoxue formula is comprised of Tu Si Zi (*Cuscutae semen*), Sang Ji Sheng (*Taxilli herba*), Xu Duan (*Dipsaci radix*), Dang Shen (*Codonopsis radix*), Bai Zhu (*Atractylodis macrocephalae* rhizoma), Dang Gui (*Angelicae sinensis radix*), Dan Shen (*Salviae miltiorrhizae radix*) and Chuan Xiong (Chuanxiong rhizoma) as granules prepared by Sichuan New Green Pharmaceutical Technology Development Co., Ltd., and was purchased from the West Branch of the First Affiliated Hospital of Anhui University of Chinese Medicine. Human β2-GP I (p2-glycoprotein-I) was obtained from Prospec-Tany TechnoGene, Ltd. PI3K, phosphorylated (p)-PI3K), AKT, p-AKT, CD31, CD34, HIF-1α, VEGF and GAPDH were purchased from Abcam. The anticardiolipin antibody (IgG) kit was sourced from Shanghai Lianshuo Biological Technology Co. Ltd (Online). LY294002 was acquired from Sigma-Aldrich and Merck KGaA.

Modeling (10). Human β2-GP-1 was dissolved in sterile PBS to achieve a concentration of 100 µg/0.25 mL. On day 1, an injection of a solution containing human β2-GP-1 and Complete Freund's Adjuvant (CFA) was administered in a 1:1 ratio (50 µL). On day 8, incomplete Freund's Adjuvant (IFA) instead of CFA was used for booster immunization (50 µL human β2-GP-1 solution mixed with IFA in a 1:1 ratio). On day 18, female and male mice were co-housed in a 2:1 ratio, and the observation of vaginal plugs was counted as day 0 of pregnancy. On day 15 of pregnancy, the pregnant mice were euthanized, their eyeballs were collected for blood sampling, and the embryo resorption rate was calculated. The placental tissue was fixed with 4% paraformaldehyde and then paraffin sections were prepared for standard pathology, TUNEL and immunohistochemical testing, while fresh placental tissue was stored at -80ºC for reverse transcription-quantitative PCR (RT-qPCR) and western blotting. Blood samples were allowed to stand at room temperature for 10 min before centrifugation at 3,000 x g for 10 min at 4°C; the supernatant was collected and stored at -20°C. Aseptic dissection was immediately performed to examine, weigh and photograph the uteri and ovaries. Finally, the tissues were isolated and rapidly placed in liquid nitrogen for storage at -80°C.

The negative control (NC) group consisted of mice undergoing normal mating and giving birth. The model, model + Bushenhuoxue formula, and model + Bushenhuoxue formula + LY294002 groups were established using the aforementioned RSA modeling procedure. In the model + Bushenhuoxue formula group, each pregnant mouse was orally administered Bushenhuoxue formula at a dose of 0.5 g (11). In the model + Bushenhuoxue formula + LY294002 group, pregnant mice were administered the same dose of Bushenhuoxue formula orally and concurrently injected with 8.0 mg/kg LY294002 (12).

The present study was approved by the Ethics Committee of Anhui Province Integrated Traditional Chinese and Western Medicine Hospital (approval no. 2022102351).

Hematoxylin and eosin (H&E) staining of placental tissues. On day 12 of pregnancy, fasting for 12 h was followed by intraperitoneal injection of 2% pentobarbital sodium (40 mg/kg) the following day by anesthesia. After anesthesia, euthanasia was performed on pregnant mice using the cervical dislocation method, and placental tissues were collected and processed through fixation, dehydration, embedding, sectioning, deparaffinization, H&E staining and rinsing for 1-20 min. Subsequent differentiation involved treating sections with 1% hydrochloric acid alcohol for 5-10 sec, followed by rinsing. Bluing was accomplished using ammonia water for 5-10 sec and staining with 0.5% eosin solution for 3-5 min. After rinsing, the sections underwent dehydration, clearing, mounting and imaging using a light microscope.

Immunofluorescence (IF) staining for CD31, CD34, HIF-1α and VEGF expression in placental tissues. Placental tissues from every group of pregnant mice were embedded in paraffin, and subsequent deparaffinization was carried out through ethanol-water cycles, alternating boiling and cooling in 5-min intervals, repeated twice. Sections were subsequently washed three times with PBS for 5 min, blocked at room temperature for 30 min, exposed to primary antibodies (CD31, 1:500, ab28364, Abcam; CD34,1:500, ab8158, Abcam; HIF-1*α*, 1:500, ab16066, Abcam; VEGF, 1:500, ab115805, Abcam) overnight at 4°C, washed three times with PBS for 5 min, incubated with Alexa Fluor 594-conjugated goat anti-rabbit secondary antibody (ImmunoWay Biotechnology Company) at 37°C for 30 min, subjected to DAPI staining for 10 min at room temperature, washed again three times with PBS for 5 min, and finally mounted. Images of placental tissues were captured using an Olympus fluorescence microscope (Olympus) and analyzed using ImageJ 1.51k software (National Institutes of Health).

Calculation of embryo loss rate. The total embryo count, viable embryo count and miscarried embryo count were recorded to calculate the embryo loss rate. The embryo loss rate (ELR) was determined using the equation: ELR (%) = (number of miscarried embryos)/(number of miscarried embryos + number of viable embryos) x 100%.

Enzyme-linked immunosorbent assay (ELISA). Frozen serum samples were thawed, and ELISA assays were conducted as per the provided kit instructions (AT-III ELISA kit, ml025687, Mlbio; PROG ELISA kit, ml057583, Mlbio; HCG ELISA kit, ml024543, Mlbio; E2 ELISA kit, ml002009, Mlbio; t-PA ELISA kit, ml037187, Mlbio; APC ELISA kit, APC ELISA kit, ml002190, Mlbio). Standard samples and serum were added to designated wells. After successive steps involving incubation, washing, antibody addition and subsequent incubation, color development occurred. Optical density was measured at 450 nm using a microplate reader. Serum concentrations of PROG (progesterone), HCG (human chorionic gonadotropin), E2 (estradiol), AT-III (antithrombin III), t-PA (tissue plasminogen activator) and APC (activated protein C) are derived from the standard curve.

Western blotting. Proteins were extracted from placental tissues using the BCA method to enable quantification. A 10% SDS-PAGE gel was prepared, followed by electrophoresis and subsequent wet transfer to a membrane. The membrane was blocked with 5% skim milk for 2 h, after which it was incubated with primary antibodies, including PI3K (1:1,000, catno. ab283852; Abcam), AKT (1:1,000, catno. ab8805, Abcam), *p*-PI3K (1:1,000, catno. ab 278545, Abcam), *p*-AKT (1:1,000 catno. ab38449, Abcam), HIF-1*α* (1:1,000, catno. ab308637, Abcam), VEGF (1:1,000, catno.ab 315238, Abcam), and GAPDH (1:1,000, catno. ab313650, Abcam) overnight at 4ºC. The next day, the membrane underwent washing with 1X TBS-0.1% Tween-20 (cat. no. 9997; Cell Signaling Technology, Inc.), followed by incubation with secondary antibodies (1:2,000) for 1 h with gentle agitation. This was succeeded by an additional 2-h incubation at room temperature. After thorough washing, visualization was achieved through exposure to enhanced chemiluminescence reagents. Band intensities were analyzed using ImageJ, with GAPDH used as the internal control.

RT-qPCR. Frozen placental tissue samples (20 mg) were pulverized using liquid nitrogen. Total RNA was extracted using the TRIzol reagent. Following RNA quantification (1 μg), cDNA synthesis was conducted using a RT kit. qPCR took place using the amplification kit and the following thermocycling conditions: 95°C pre-denaturation for 30 sec, denaturation at 95°C for 5 sec and annealing at 60°C for 30 sec, totaling 40 cycles. The relative expression level of the target gene was computed using the $2^{-\Delta\Delta Ct}$ method (13) with GAPDH serving as the reference gene. Primer sequences were provided by Beijing Lainuo BioTech Co., Ltd (Table 1).

TABLE 1 - Primer sequence

Gene Name	F:(5'-3')	R:(5'-3')
PI3K	ACGACTACAAGAAGGAGCGAG	CAGCCAATATCTTCAGGCCG
AKT	GGACAACCGCCATCCAGACT	GCCAGGGACACCTCCATCTC
HIF-1α	GGATGAGTTCTGAACGTCGAAAAG	ACATTGTGGGGAAGTGGCAA
VEGF	ATGAACTTTCTGCTGTCTTGG	TCACCG CCTCGGCTTGTCACA
U6	CTCGCTTCGGCAGCACA	AACGCTTCACGAATTTGCGT
GAPDH	GGTGAAGGTCGGTGTGAACG	GCTCCTGGAAGATGGTGATGG

TUNEL staining. Paraffin-embedded placental tissues were sectioned to 5-µm-thick slices on glass slides after fixation in 4% paraformaldehyde. TUNEL fluorescence detection was carried out according to the manufacturer's instructions. After PBS buffer washing, cell nuclei were re-stained with DAPI. Slides were incubated at room temperature for 2 min before mounting. The sections were observed and imaged using a fluorescence microscope and TUNEL$^+$ cells were counted.

Statistical analysis. SPSS (version 23.0; IBM Corp.) was used for statistical analysis. Normally distributed measurement data were presented as mean ± standard deviation. Group comparisons were conducted through analysis of variance, and homogeneity of variance was determined using the LSD test for equal variances or the Games-Howell test for unequal variances. P<0.05 was considered to indicate a statistically significant difference.

Results

Network pharmacology. The GSE26787 dataset encompassed gene data from five RSA placental tissues and five placental tissues from normal deliveries. Subsequent analysis unveiled a total of 2,169 differentially expressed genes. Among these, 1,061 genes were underexpressed in RSA placental tissues, while 1,108 genes were overexpressed. A volcano plot was generated accordingly (Fig. 1A), and the top 20 genes with the most significant differential expression in both categories were selected for further investigation. To visually represent these findings, a heatmap was plotted (Fig. 1B). Through the GeneCards database analysis, it was identified that 2,169 targets were linked to RSA, while 195 targets were connected to the efficacious components of the Bushenhuoxue formula. Among these, 20 targets were identified as shared between Bushenhuoxue formula constituents and the disease (Fig.2). Relative data including active ingredient, targeting gene loci and disease targeting gene loci were collected. A 'Drug constituent-shared target' network was built using Cytoscape (Fig. 3). The CytoNCA tool was used to compute the degree, betweenness centrality, and closeness centrality of the targets, thereby pinpointing the most pivotal components (Fig. 3). The interactions among the 20 shared targets were elucidated by STRING database analysis (https://www.string-db.org/; version 11.5), and the outcomes were depicted *via* Cytoscape, resulting in the creation of a PPI network (Fig. 4). As revealed by the PPI network analysis, the PI3K target exhibited the greatest potential for therapeutic intervention. DAVID was used to conduct GO functional enrichment analysis, and the significance threshold was set at P<0.05. The top 20 entries with the highest gene counts are shown in Fig. 5. For BP, the most prominent term was 'regulation of response to wounding'. In terms of CC, a significant association was observed with 'plasma membrane raft', while MF was primarily linked to 'steroid binding'. KEGG pathway enrichment analysis was conducted using DAVID with a significance threshold of P<0.05. A total of 22 enriched pathways were identified and ranked by gene count (Fig. 6). The five most enriched pathways were 'cellular senescence', 'chemical carcinogenesis - receptor activation', 'p53 signaling pathway', 'HIF-1 signaling pathway'and 'linoleic acid metabolism'.

Intergroup comparison of embryo loss rates. Compared with the NC group, the model group exhibited a significantly increased embryo loss rate (P<0.05). By contrast, the model + Bushenhuoxue formula group demonstrated a significant reduction in embryo loss rate compared with the model group (P<0.05). However, when simultaneous LY294002 intervention was introduced, the model + Bushenhuoxue formula + LY294002 group displayed a significant increase in embryo loss rate compared with the model + Bushenhuoxue formula group (P<0.05; Table 2).

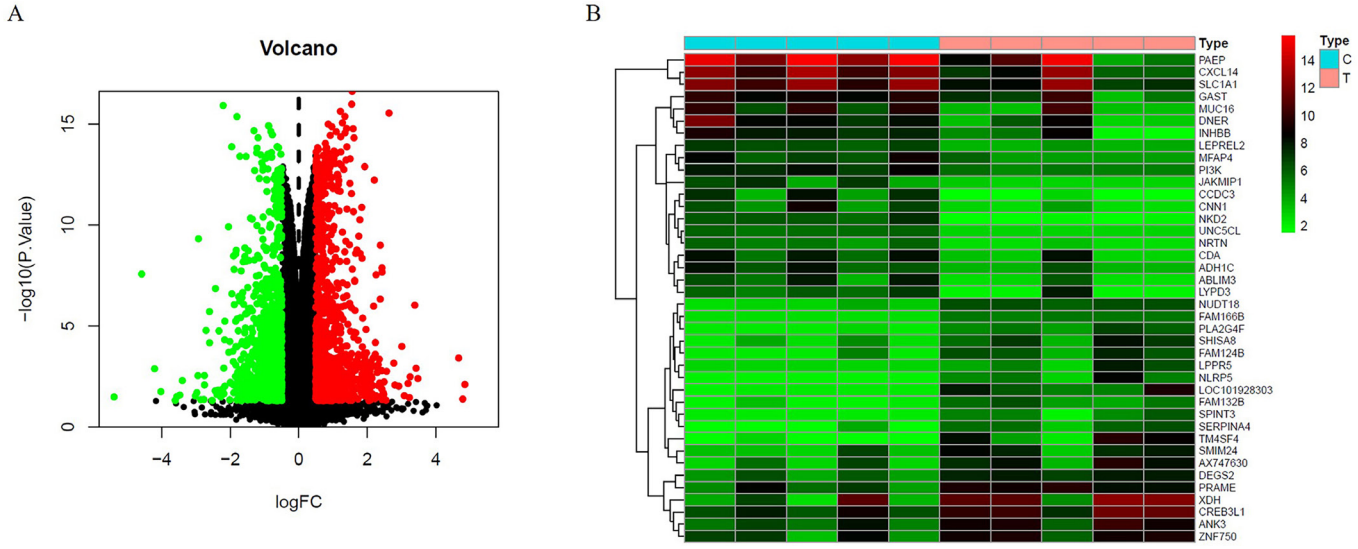

FIGURE 1 - Differential gene expression analysis in RSA. (A) volcano plot and (B) heart map.

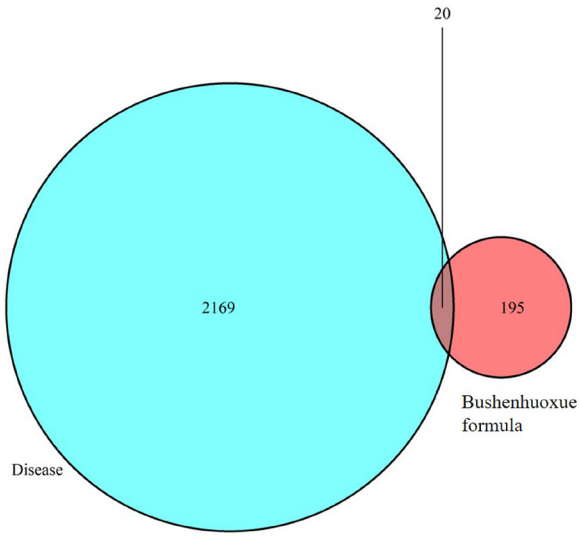

FIGURE 2 - Intersection of Bushenhuoxue formula constituent targets and RSA-related targets. RSA, recurrent spontaneous abortion.

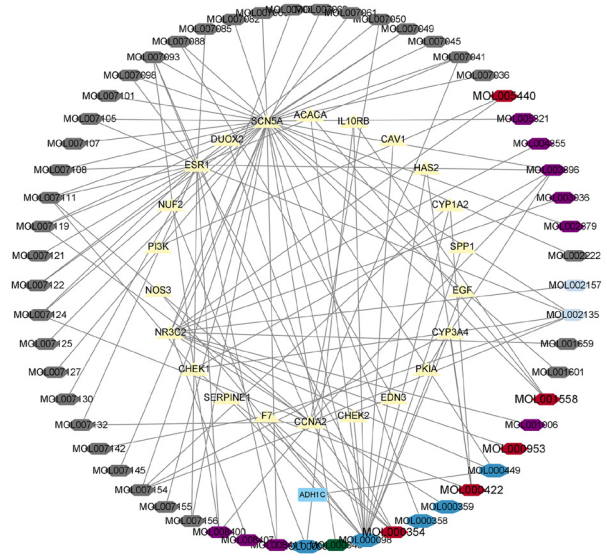

FIGURE 3 - Analysis of Bushenhuoxue formula constituent-target network.

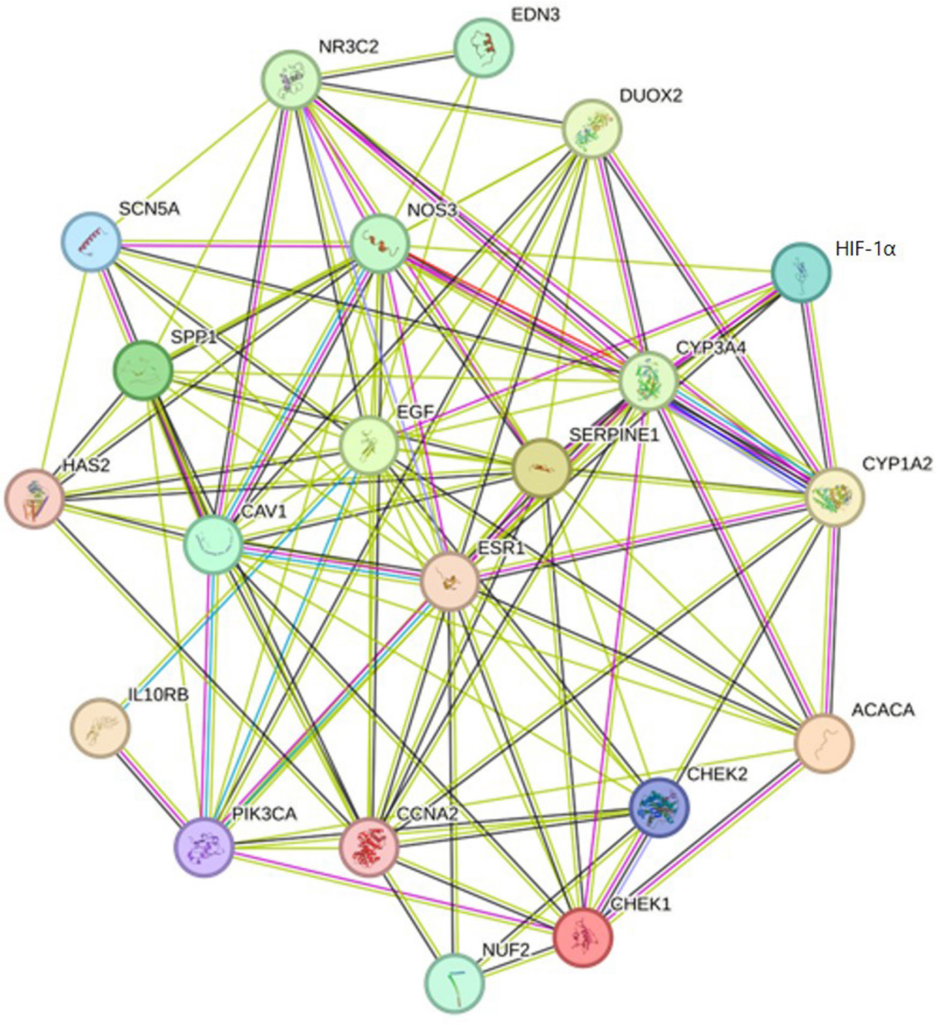

FIGURE 4 - Protein-protein interaction network analysis of shared target interactions.

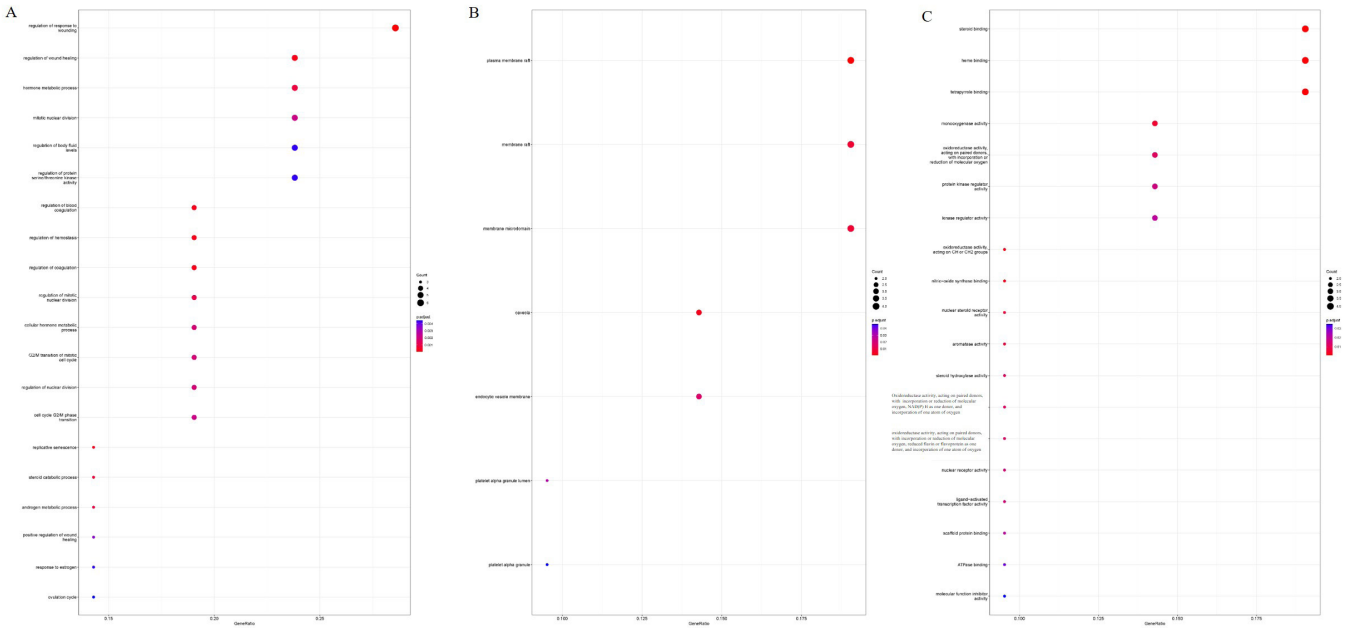

FIGURE 5 - Enrichment analysis of shared targets in Gene Ontology terms. (A) BP, (B) CC and (C) MF. BP, biological process; MF, molecular function; CC, cellular component. (Also available as supplementary figure A).

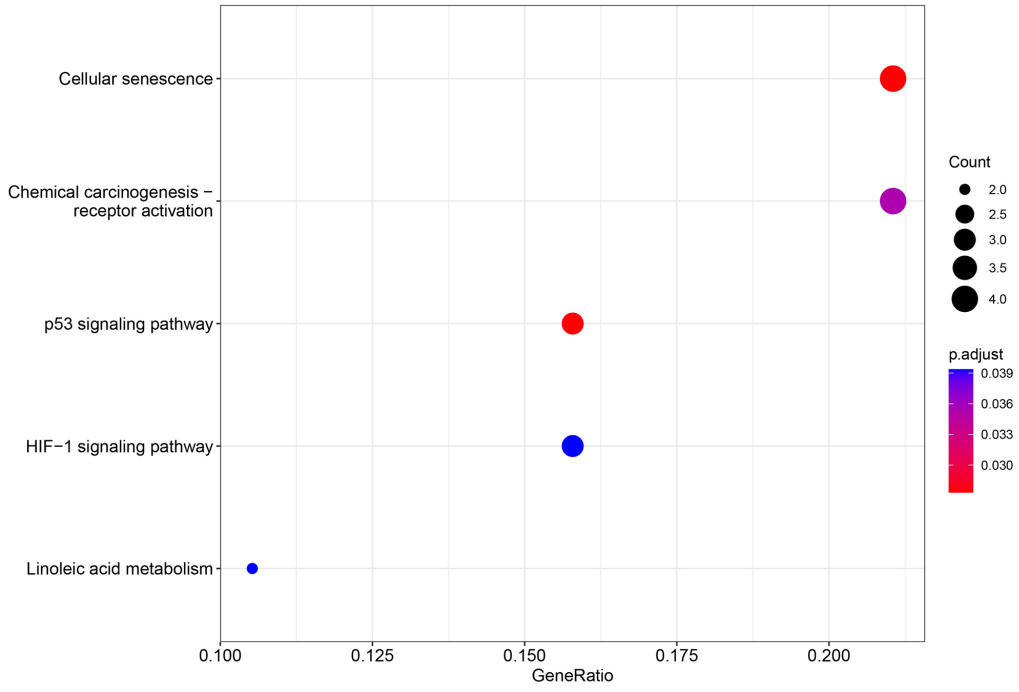

FIGURE 6 - Kyoto Encyclopedia of Genes and Genomes enrichment analysis of shared targets.

TABLE 2 - Comparison of embryo loss rate in each group (Mean±SD, n = 9)

Group	Total number of embryos	Number of aborted embryos	ELR(%)
NC	54	5	5.76±4.84
Model	86	23	25.95±8.54*
Model+Drug	81	12	10.57±6.19#
Model+Drug+LY294002	85	22	24.95±7.16@

*:P<0.05, compared with NC; #: P<0.05, compared with Model; @: P<0.05, compared with Model+Drug

Intergroup comparison of serum hormone levels and coagulation factor levels. In comparison with the NC group, the model group exhibited a significant decrease in the serum levels of AT-III, t-PA, P, APC and HCG (all P<0.05; Fig. 7). Conversely, the model + Bushenhuoxue formula group demonstrated significantly elevated levels of serum AT-III, t-PA, P, APC and HCG compared with the model group (all P<0.05; Fig. 7). Notably, with the administration of LY294002, the model + Bushenhuoxue formula + LY294002 group exhibited a significant rise in the serum levels of AT-III, t-PA, P, APC and HCG compared with the model + Bushenhuoxue formula group (all P<0.05; Fig. 7).

Comparison of pathological morphological changes in placental regions. The H&E staining results (Fig. 8A) revealed distinct variations in placental tissue morphology among different groups. In the NC group, the decidua, and the syncytiotrophoblast and labyrinth layers exhibited normative structures. Compared with the NC group, the model group demonstrated partial shedding of the decidua, along with syncytiotrophoblast necrosis characterized by diminished numbers, focal necrosis in the labyrinth layer and notable infiltration of inflammatory cells. By contrast, the model + Bushenhuoxue formula group presented well-defined structures across all placental layers, featuring only focal necrosis in the labyrinth layer and minimal inflammatory cell infiltration. Notably, other structures displayed no significant pathological changes. However, concurrent administration of LY294002 nullified the therapeutic effects of the Bushenhuoxue formula.

Comparison of changes in apoptosis of placental tissues. Evaluation of TUNEL staining outcomes disclosed that compared with the NC group, the model group exhibited a significant increase in TUNEL$^+$ apoptotic cells (P<0.05; Fig. 8B). Introducing Bushenhuoxue formula intervention, the model + Bushenhuoxue formula group showcased a significant reduction in the number of TUNEL$^+$ apoptotic cells compared with the model group (P<0.05; Fig. 8B). Nonetheless, the simultaneous application of LY294002 yielded a marked increase in the tally of TUNEL$^+$ apoptotic cells in the model + Bushenhuoxue formula + LY294002 group compared with the model + Bushenhuoxue formula group (P<0.05; Fig. 8B).

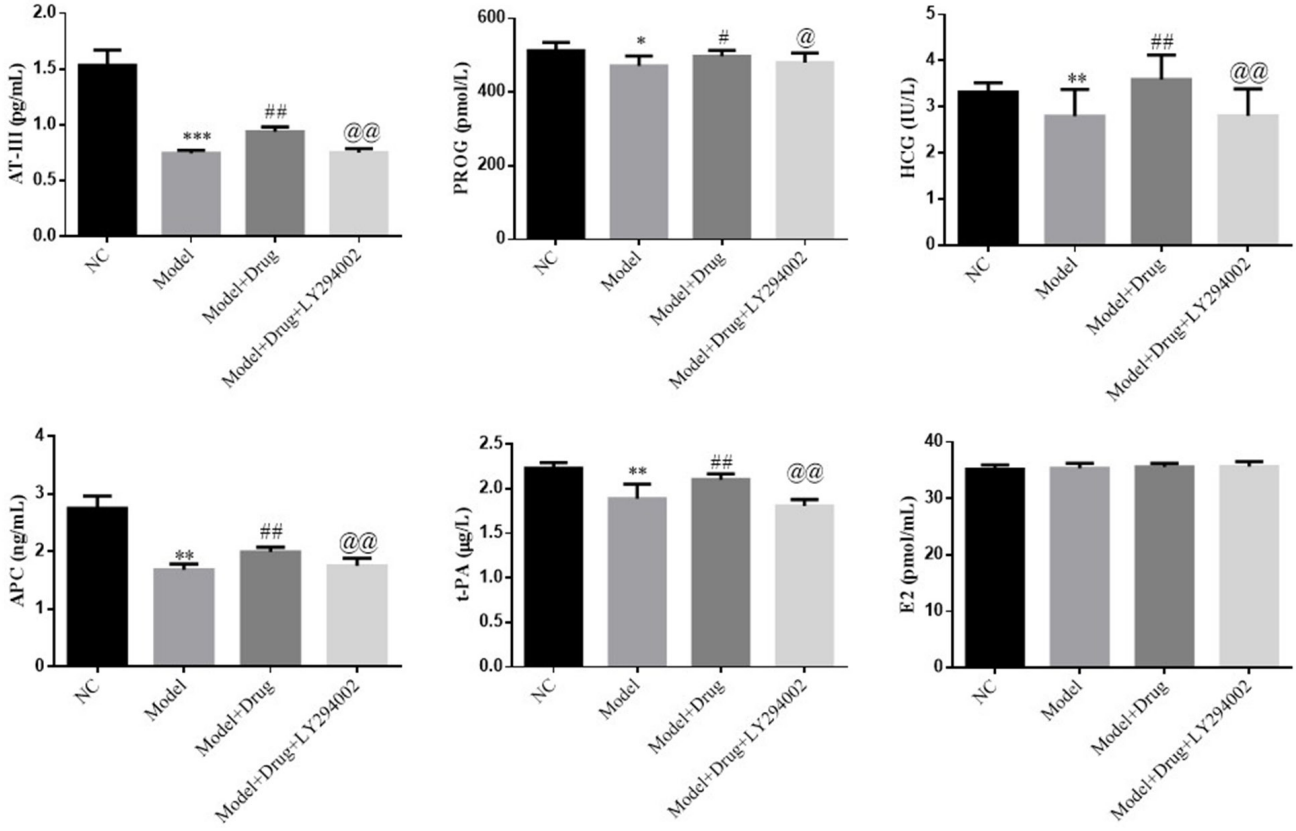

FIGURE 7 - Intergroup comparison of serum hormone levels and coagulation factor levels.
*P<0.05, **P<0.01, ***P<0.001, compared with the NC group; #P<0.05, ##P<0.01, compared with the model group; @P<0.05, @@P< 0.01, compared with the model + Bushenhuoxue formula group. NC, negative control

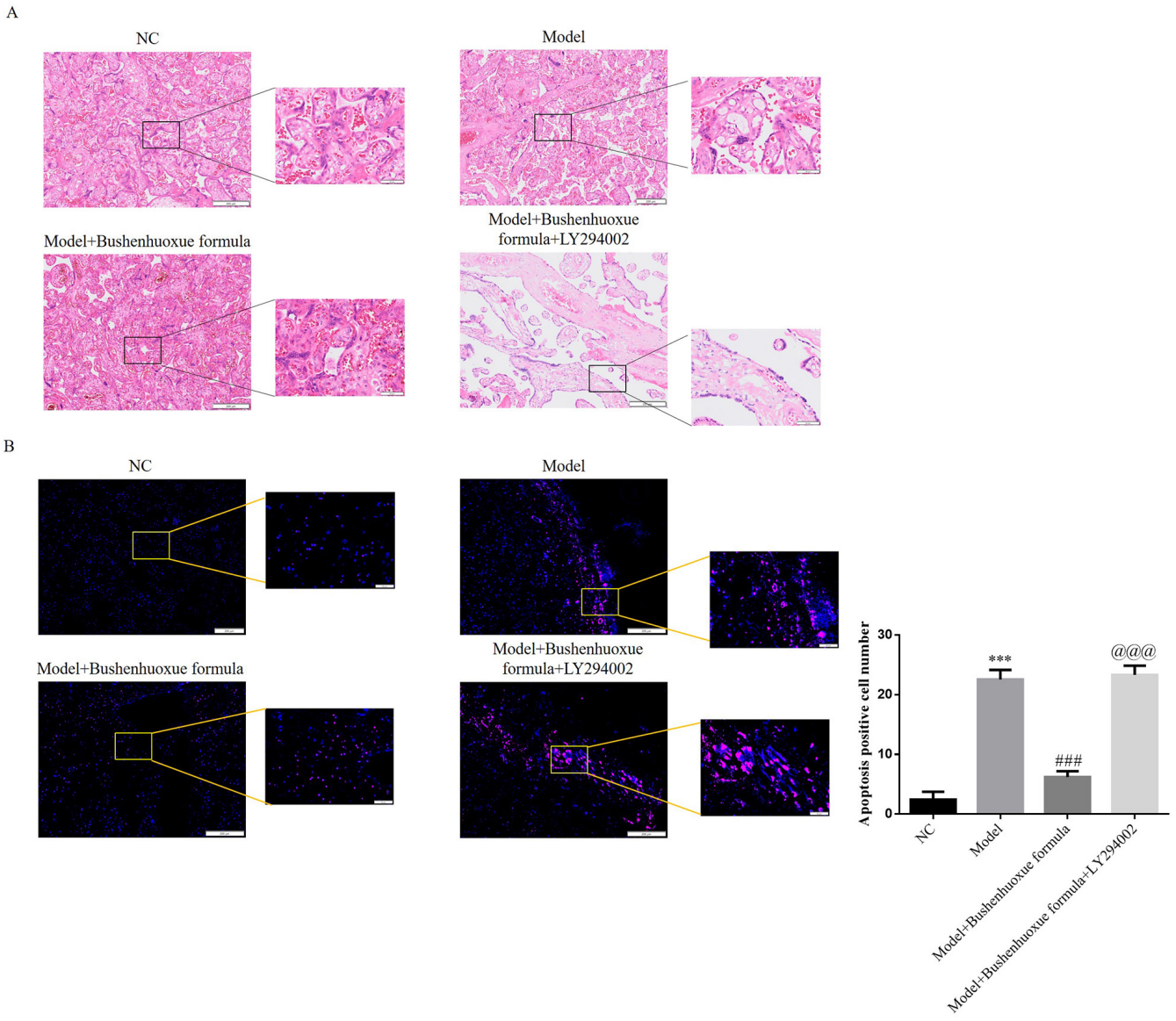

FIGURE 8 - Pathological changes in each group.
A. Comparison of pathological morphological changes in placental regions using H&E staining (magnification, x100; scar bar, 200μm; magnification, x400; scar bar, 200μm); B. Comparison of changes in apoptosis of placental tissues using TUNEL assay (magnification, x100; scar bar, 200μm; magnification, x400; scar bar, 200μm). ***P<0.001, compared with the NC group; ###P<0.001, compared with the model group; @@@P<0.001, compared with the model + Bushenhuoxue formula group. NC, negative control

Comparison of CD31 and CD34 protein expression in placental tissues. IHC analysis showed that compared with the NC group, the model group exhibited significantly reduced levels of CD31 and CD34 protein expression (P<0.05; Figs. 9A and 9B). On the other hand, subsequent Bushenhuoxue formula intervention in the model + Bushenhuoxue formula group elicited significantly heightened levels of CD31 and CD34 protein expression contrary to the model group (P<0.05; Figs. 9A and 9B). The concurrent administration of LY294002 led to a significant reduction in CD31 and CD34 protein expression levels within the model + Bushenhuoxue formula + LY294002 group compared with the model + Bushenhuoxue formula group (P<0.05; Figs. 9A and 9B).

Comparison of relevant gene expression in placental tissues. RT-qPCR revealed that compared with the NC group, the model group exhibited a significant reduction in the gene expression levels of PI3K, AKT, HIF-1α and VEGF (all P<0.001; Fig. 9C). Subsequent intervention with Bushenhuoxue formula in the model + Bushenhuoxue formula group prompted a significant increase in the gene expression levels of PI3K, AKT, HIF-1α and VEGF when compared with the model group (all P<0.001; Fig. 9C). Nevertheless, simultaneous administration of LY294002 resulted in a significant decrease in the gene expression levels of PI3K, AKT, HIF-1α and VEGF within the model + Bushenhuoxue formula + LY294002 group compared with the model + Bushenhuoxue formula group (all P<0.001; Fig. 9C).

Comparison of relevant protein expression in placental tissues. Western blotting showed that compared with the NC group, the model group exhibited a significant decrease in the protein expression levels of *p*-PI3K/PI3K, p-AKT/AKT, HIF-1*α* and VEGF (all P<0.001; Fig. 9D). Introducing the Bushenhuoxue formula in the model + Bushenhuoxue formula group led to a significant escalation in the protein expression levels of *p*-PI3K/PI3K, *p*-AKT/AKT, HIF-1*α* and VEGF compared with the model group (all P<0.001; Fig. 9D). Nonetheless, simultaneous administration of LY294002 yielded a significant decrease in the protein expression levels of p-PI3K/PI3K, p-AKT/AKT, HIF-1*α* and VEGF within the model + Bushenhuoxue formula + LY294002 group contrary to the model + Bushenhuoxue formula group (all P<0.001; Fig. 9D).

Comparison of HIF-1α and VEGF protein expression in placental tissues. The IHC analysis showed that compared with the NC group, the model group demonstrated a significant reduction in HIF-1*α* and VEGF protein expression (P<0.001; Fig. 9E and 9F). By contrast, the administration of the Bushenhuoxue formula in the model + Bushenhuoxue formula group led to significant elevations in HIF-1*α* and VEGF protein expression compared with the model group (P<0.001; Fig. 9E and 9F). However, the concurrent administration of LY294002 resulted in a significant reduction in HIF-1*α* and VEGF protein expression levels in the model + Bushenhuoxue formula + LY294002 group compared with the model + Bushenhuoxue formula group (P<0.001; Fig. 9E and 9F).

Discussion

RSA is a prevalent reproductive disorder affecting women of childbearing age, with the etiology of 50-60% of the cases remaining ambiguous. In light of its intricate pathogenesis and the significant challenges in treatment, RSA has emerged as a notable research domain in recent years (14, 15). From the implantation of a fertilized egg to childbirth, a delicate equilibrium between heightened coagulability and augmented vulnerability to bleeding is meticulously upheld. Disturbance to this equilibrium can wield profound impacts on crucial processes, including fertilized egg implantation, establishment of pathological placenta and even miscarriage (16). The intimate nexus between ACA and RSA has gathered increasing attention. Earlier investigations predominantly ascribed the pathogenesis of ACA provoking vascular thrombosis and tissue infarction at the placental locale, resulting in harm to placental vascular epithelial cells. However, subsequent studies have shown that thrombosis alone may not be the sole causative factor (17, 18). Anti-phospholipid antibodies can engage directly with trophoblast phospholipids, triggering apoptosis, fostering coagulation cascades and inciting unbridled immune responses. These antibodies also hinder the differentiation and maturation of trophoblasts, engendering compromised syncytiotrophoblast fusion. This compromise in turn impairs HCG synthesis, curtails trophoblast invasiveness and derails uterine spiral artery remodeling, thus resulting in trophoblast impairment, apoptosis and thwarted embryo implantation (19). Our previous study showed that the Bushenhuoxue formula had effects to improve recurrent miscarriage (20). However, there were some tractions from Bushenhuoxue formula; the mechanism has been unclear, and based on the results it was decided to investigate the mechanism using network pharmacology and *in vivo* study for validation. In the present study, it was shown that the Bushenhuoxue formula had treatment effects through regulation of the PI3K/AKT pathway based on network pharmacology analysis; the data were validated through animal experiments.

The PI3K/AKT signaling pathway is a marked cellular mechanism governing the intricate orchestration of cell proliferation, apoptosis and the cell cycle (16). Activation of the PI3K/AKT pathway can enhance cell proliferation and suppress apoptosis. PI3K, positioned as a cardinal upstream molecule within the PI3K/AKT/HIF-1*α* pathway, spurs p110*α* enzyme activity through its subunit PIK3CA, thereby inciting cell growth that operates autonomously from external growth factors (21). AKT, serving as a crucial downstream effector of PI3K, and its activated variant, p-AKT, can phosphorylate an array of components closely interlinked with apoptosis, thus fostering cellular survival (22). As an ensuing cascade of the PI3K/AKT pathway (23, 24), the HIF-1*α*/VEGF signaling pathway holds promise in angiogenesis and the amelioration of hemostatic conditions (25, 26). In the current study, the methodology of network pharmacology was harnessed to dissect the plausible mechanisms underlying the influence of Bushenhuoxue formula on the prothrombotic state associated with RSA. The results cogently suggested that the formula may enact its effects through the activation of the PI3K/AKT signaling pathway. To substantiate this proposition, animal experiments were conducted, the findings of which affirmed that the formula efficaciously triggers the PI3K/AKT signaling pathway, thereby subsequently engaging the downstream HIF-1*α*/VEGF pathway. This sequence of activations ushers in elevated levels of serum AT-III, t-PA, P, APC and HCG, thereby furnishing robust protection against RSA. Furthermore, the formula was shown to mitigate trophoblast apoptosis, and escalate vascular density, as indicated by the increased CD34 and CD31 protein expression (27, 28). However, it is noteworthy that the therapeutic efficacy of the Bushenhuoxue formula rendered void in the presence of LY294002, a PI3K inhibitor .

Conclusion

The combined findings stemming from network pharmacology analysis and animal experimentation coalesce to portray that the Bushenhuoxue formula has the propensity to activate the PI3K/AKT signaling pathway. This activation curtails trophoblast apoptosis induced by RSA, while the orchestration of the downstream HIF-1*α*/VEGF pathway engenders a mitigation of the prothrombotic state and fosters vasculogenesis, thereby achieving robust fortification against RSA. There were some limitations in the present study; we just discussed the Bushenhuoxue formula's treatment effects *in vivo* study, the clearly mechanism has been unclear. In future research, this limitation will be addressed by carrying out *in vitro* experiments.

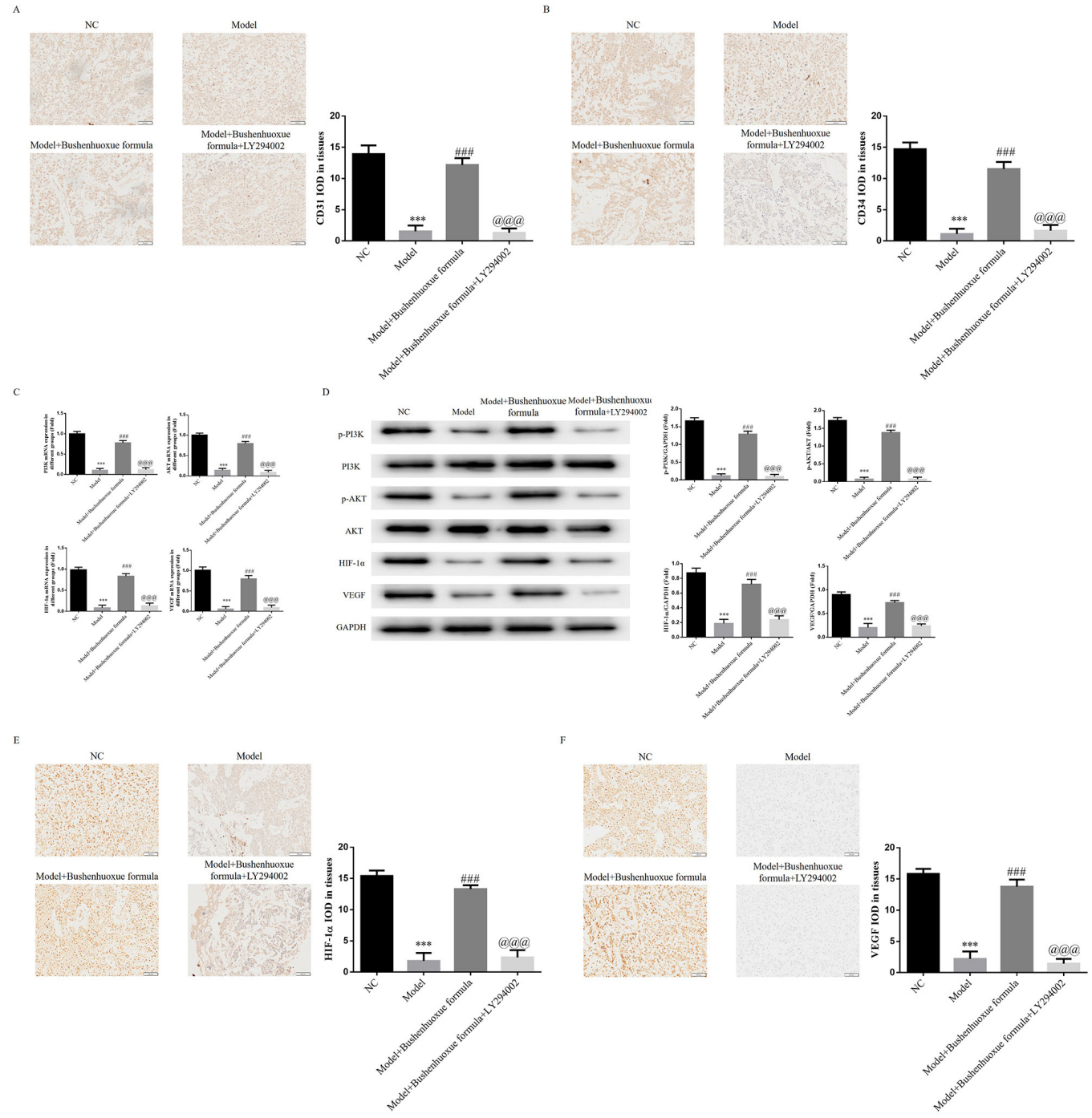

FIGURE 9 - Relative mRNA and Protein expression.
A. CD31 protein expression in placental tissues using immunohistochemistry (magnification, x100; scar bar, 100μm). ***P<0.001, compared with the NC group; ###P<0.001, compared with the model group; @@@P<0.001, compared with model + Bushenhuoxue formula group. NC, negative control; B. CD34 protein expression in placental tissues using immunohistochemistry (magnification, x100; scar bar, 100μm). ***P<0.001, compared with the NC group; ###P<0.001, compared with the model group; @@@P<0.001, compared with model + Bushenhuoxue formula group. NC, negative control; C. Comparison of relevant gene expression in placental tissues (magnification, x100). ***P<0.001, compared with the NC group; ###P<0.001, compared with the model group; @@@P<0.001, compared with model + Bushenhuoxue formula group. NC, negative control; D. Relative proteins expression in placenta tissues using western blotting. ***P<0.001, compared with the NC group; ###P<0.001, compared with the model group; @@@P<0.001, compared with model + Bushenhuoxue formula group. NC, negative control; E. HIF-1α protein expression in placental tissues using immunohistochemistry (magnification, x100; scar bar, 100μm). ***P<0.001, compared with the NC group; ###P<0.001, compared with the model group; @@@P<0.001, compared with model + Bushenhuoxue formula group. NC, negative control; F. VEGF protein expression in placental tissues using immunohistochemistry (magnification, x100; scar bar, 100μm). ***P<0.001, compared with the NC group; ###P<0.001, compared with the model group; @@@P<0.001, compared with model + Bushenhuoxue formula group. NC, negative control.

Disclosures

Conflict of interest: The authors declare that they have no competing interests.

Financial support: The present study was funded by the Anhui Province Higher Education Science Research Project (gran no. 2022AH050443) and the Anhui Red Cross Society Traditional Chinese medicine inheritance innovation development research project (grant no. 2022ZYYD08).

Authors' contributions: XY and SLS designed the study, performed the experiments, analyzed and interpreted the data and wrote the manuscript. LJL, PL, MQL, YNW and YQG collected samples and clinical data, analyzed and interpreted the data, and wrote the manuscript. LJL and PL provided and analyzed the samples, and interpreted the results and clinical data of the patients. MQL, YNW and YQG confirm the authenticity of all the raw data. All authors have read and approved the final version of the manuscript.

Data availability statement: The datasets used and/or analyzed during the current study are available from the corresponding author on reasonable request.

Ethics approval and consent to participate: The present study was approved by the Ethics Committee of Shanghai University of Traditional Chinese Medicine affiliated Shuguang Hospital Anhui Hospital (approval no. 2022102351).

References

1. Wang F, Jia W, Fan M, et al. Single-cell Immune Landscape of Human Recurrent Miscarriage. Genomics Proteomics Bioinformatics. 2021;19(2):208-222. CrossRef PubMed
2. Tian Y, Fu Z, Lan H, et al. Chinese traditional herbs enhanced the clinical efficacy of low-molecular-weight heparin in the treatment of recurrent spontaneous abortion complicated with thrombophilia. Heliyon. 2023;9(2):e13120. CrossRef PubMed
3. Wang X, Zhao Y, Zhong X. Protective effects of baicalin on decidua cells of LPS-induced mice abortion. J Immunol Res. 2014;2014:859812. CrossRef PubMed
4. Lin P, Ji HH, Li YJ, Guo SD. Macrophage Plasticity and Atherosclerosis Therapy. Front Mol Biosci. 2021;8:679797. CrossRef PubMed
5. Svensson-Arvelund J, Ernerudh J, Buse E, et al. The placenta in toxicology. Part II: systemic and local immune adaptations in pregnancy. Toxicol Pathol. 2014;42(2):327-338. CrossRef PubMed
6. Li J, Feng D, He S, Wu Q, Su Z, Ye H. Meta-analysis: association of homocysteine with recurrent spontaneous abortion. Women Health. 2021;61(7):713-720. CrossRef PubMed
7. Liu Z, Sun S, Xu H, et al. Prognostic analysis of antibody typing and treatment for antiphospholipid syndrome-related recurrent spontaneous abortion. Int J Gynaecol Obstet. 2022;156(1):107-111. CrossRef PubMed
8. Song Y, Zhou F, Tan X, et al. Bushen Huoxue recipe attenuates early pregnancy loss via activating endometrial COX2-PGE2 angiogenic signaling in mice. BMC Complement Med Ther. 2021;21(1):36. CrossRef PubMed
9. Zhao J, Chen P, Xu G, et al. [Bushen Huoxue Fang improves recurrent miscarriage in mice by down-regulating the JAK2/STAT3 pathway]. Nan Fang Yi Ke Da Xue Xue Bao. 2023;43(2):265-270. PubMed
10. Katzav A, Menache zm A, Maggio N, Pollak L, Pick CG, Chapman J. IgG accumulates in inhibitory hippocampal neurons of experimental antiphospholipid syndrome. J Autoimmun. 2014;55:86-93. CrossRef PubMed
11. Luo S, Jing J, Zhang Y, Yu W, Gao W. Network pharmacology and the experimental findings of Bushenhuoxue formula for improving hippocampal neuron injury in vascular demented rats. J Integr Neurosci. 2021;20(4):847-859. CrossRef PubMed
12. Cai Q, Li Q, Zhong S, et al. Ultrasound-targeted microbubble destruction rapidly improves left ventricular function in rats with ischemic cardiac dysfunction. Int J Cardiol. 2024;404:131943. CrossRef PubMed
13. Livak KJ, Schmittgen TD. Analysis of relative gene expression data using real-time quantitative PCR and the 2(-Delta Delta C(T)) Method. Methods. 2001;25(4):402-408. PMID:CrossRef PubMed
14. Reddel HK, Bacharier LB, Bateman ED, et al. Global Initiative for Asthma Strategy 2021: executive summary and rationale for key changes. Eur Respir J. 2021;59(1):2102730. CrossRef PubMed
15. Grandone E, Tiscia GL, Mastroianno M, et al. Findings from a multicentre, observational study on reproductive outcomes in women with unexplained recurrent pregnancy loss: the OTTILIA registry. Hum Reprod. 2021;36(8):2083-2090. CrossRef PubMed
16. Liu X, Chen Y, Ye C, Xing D, Wu R, Li F, Chen L, Wang T. Hereditary thrombophilia and recurrent pregnancy loss: a systematic review and meta-analysis. Hum Reprod. 2021 20;36(5):1213-1229. CrossRef
17. Al Jameil N, Tyagi P, Al Shenefy A. Incidence of anticardiolipin antibodies and lupus anticoagulant factor among women experiencing unexplained recurrent abortion and intrauterine fetal death. *Int J Clin Exp Pathol*. 2015;8(3):3204-3209. PubMed
18. Bose P, Black S, Kadyrov M, et al. Adverse effects of lupus anticoagulant positive blood sera on placental viability can be prevented by heparin in vitro. *Am J Obstet Gynecol*. 2004;191(6):2125-2131. CrossRef PubMed
19. Sung N, Khan SA, Yiu ME, et al. Reproductive outcomes of women with recurrent pregnancy losses and repeated implantation failures are significantly improved with immunomodulatory treatment. *J Reprod Immunol*. 2021;148:103369. CrossRef PubMed
20. Yang X, Su S, Ren Q, et al. BushenHuoxue Recipe for the Treatment of Prethrombotic State of ACA-Positive Recurrent Miscarriage via the Regulation of the PI3K-AKT Signaling Pathway. *Evid Based Complement Alternat Med*. 2022;2022:2385534. CrossRef PubMed
21. García-Escudero R, Segrelles C, Dueñas M, et al. Overexpression of PIK3CA in head and neck squamous cell carcinoma is associated with poor outcome and activation of the YAP pathway. *Oral Oncol*. 2018;79:55-63. CrossRef PubMed
22. del Peso L, González-García M, Page C, Herrera R, Nuñez G. Interleukin-3-induced phosphorylation of BAD through the protein kinase Akt. *Science*. 1997;278(5338):687-689. CrossRef PubMed
23. Xie W, Zhou P, Qu M, et al. Corrigendum: Ginsenoside Re Attenuates High Glucose-Induced RF/6A Injury *via* Regulating PI3K/AKT Inhibited HIF-1a/VEGF Signaling Pathway. *Front Pharmacol*. 2020;11:1312. CrossRef PubMed
24. Tayler HM, MacLachlan R, Güzel Ö, Miners JS, Love S. Elevated late-life blood pressure may maintain brain oxygenation and slow amyloid-β accumulation at the expense of cerebral vascular damage. Brain Communications. 2023 ;5(2):fcad112. CrossRef PubMed
25. Li H, Zhao B, Liu Y, Deng W, Zhang Y. Angiogenesis in residual cancer and roles of HIF-1α, VEGF, and MMP-9 in the development of residual cancer after radiofrequency ablation and surgical resection in rabbits with liver cancer. *Folia Morphol (Warsz)*. 2020;79(1):71-78. PubMed

26. Wu YF, Jin KY, Wang DP, et al. VEGF loaded nanofiber membranes inhibit chronic cerebral hypoperfusion-induced cognitive dysfunction by promoting HIF-1a/VEGF mediated angiogenesis. *Nanomedicine*. 2023;48:102639. CrossRef PubMed
27. Pusztaszeri MP, Seelentag W, Bosman FT. Immunohistochemical expression of endothelial markers CD31, CD34, von Willebrand factor, and Fli-1 in normal human tissues. *J Histochem Cytochem*. 2006;54(4):385-395. CrossRef PubMed
28. Luczynska E, Niemiec J, Ambicka A, et al. Correlation between blood and lymphatic vessel density and results of contrast-enhanced spectral mammography. *Pol J Pathol*. 2015;66(3):310-322. CrossRef PubMed